

Synthesis and Structural Characterization of Ni doped ZnSe Nanoparticles

D. Subramanyam¹, B. Hymavathi², B. Rajesh Kumar^{3*}

¹ Department of Physics, Loyola Degree College (YSRR), Pulivendula-516 390, A.P, India

²Department of Physics, Anil Neerukonda Institute of Technology (Autonomous), Visakhapatnam-531162, A.P, India

³Department of Physics, GITAM (Deemed to be University), Visakhapatnam - 530 045, A.P, India

*Email address: rajphyind@gmail.com

Abstract—In the present work synthesis of pure and Ni (5% and 10 %) doped ZnSe nanoparticles using a chemical co-precipitation method has been discussed. X-ray diffraction patterns show that the diffracted peaks are well matched with the standard powder diffraction data and exhibits cubic structure. The average crystallite size of Ni doped ZnSe nanoparticles estimated from Scherer formula are in the range of 40-67 nm. Micro structural parameters such as microstrain, dislocation density and average internal stress were estimated from X-ray diffraction data. Surface morphology and elemental analysis of the prepared samples were characterized by scanning electron microscope and energy dispersive analysis.

Keywords—II-VI semiconductors; ZnSe, X-ray diffraction; Structural properties.

I. INTRODUCTION

Wide band gap II – VI semiconductors are the novel materials for the optoelectronic device applications. The nano sized semiconductor crystallites can change optical properties which are different from bulk materials [1, 2]. Zinc selenide (ZnSe) is an n-type semiconducting material with wideband gap of 2.7 eV and large exciton binding energy of 21 meV, which is a promising candidate for nonlinear optical devices, flat panel displays, light emitting diodes, lasers, logic gates, transistors, etc.[3-5]. ZnSe nanoparticles had a wide range of applications in laser, optical instruments, etc. because of its transmittance range (0.5–22 μ m), Bohr radius as 3.8 nm at room temperature, high luminescence efficiency, low absorption coefficient and excellent transparency to infrared [6-8]. In addition, these Cd-free materials are believed to be good candidates for biomedical labelling and for using in active regions of advanced optoelectronic devices.

The doping of transition metals in group II–VI semiconductor nanomaterials depends on the chemical properties such as valence state and ionic radius between host and dopant material (metal). Compared with the rare earth ions, the doping of transition metal ions has been demonstrated to be more successful. In ZnSe, host materials in which a small atomic percentage of transition metal ions replace the cation sites in the host lattice. Transition metal elements have been successfully employed as dopants in ZnSe such as V, Cu, Mn and Ni. Ni is an important dopant in the magnetic materials. Nickel (II) is a transition metal that represents an option as dopant agent for Zn-based compound semiconductors because its atomic radius differs within the 10% limit (8.3% of difference) to Zn²⁺ radius. Therefore, the substitution of Zn²⁺ atoms by Ni²⁺ atoms in the lattice is possible [9]. Furthermore, Ni²⁺ (0.69 Å) has the same valence compared with Zn²⁺ and its radius is close to Zn²⁺ (0.74 Å), so it is possible for Ni²⁺ to replace Zn²⁺ in ZnSe lattice. Several methods such as electron beam evaporation [10,11], thermal

evaporation [12], chemical vapour deposition (CVD) [13], atomic layer deposition [14], electrodeposition [15], sol-gel method [16], etc are identified for the fabrication of ZnSe nanoparticles. Among all, wet chemical precipitation method has reported as widely acceptable method due to its features such as cost effectiveness, particle stability, versatility, less complexity, easy doping. In this paper, the influence of Ni doping on the structural and surface morphological of ZnSe nanoparticles were discussed.

II. EXPERIMENTAL DETAILS

In the present work, pure and Ni doped ZnSe nanoparticles were prepared by colloidal chemical co-precipitation method using zinc acetate, sodium selenide and nickel acetate as starting compounds. Appropriate quantities of these were weighed in a microbalance (M/s SICO, India) according to the stoichiometry to obtain 5 and 10 at% target dopant concentrations and were dissolved in 100 ml of methanol to make 0.1M solutions. The stoichiometric solution was taken in a burette and was added in drops with continuous stirring to a mixture of Na₂Se(0.1M) +1.1 ml of thiophenol + 100 ml of methanol + 50ml of H₂O until fine precipitate of ZnSe:Ni was formed. After complete precipitation, the solution in conical flask was constantly stirred for 24 hours. A single step chemical reaction is given below for the precipitation of Ni doped CdSe nanoparticles. Then the precipitates were filtered out separately and washed thoroughly with de-ionized water. Finally these samples are subjected to sintering process. The samples were calcined at 300 °C/2hrs in a vacuum. X-ray diffraction (XRD) patterns have been recorded over the range of 10° - 80° at the scan rate of 2°/min using Powder X-ray diffractometer (Model: SIEFERT 3003 TT) with CuK α ($\lambda=1.5420$ Å) as target material. Surface morphology and compositional analysis of the samples has been studied using Field emission scanning electron microscope (FESEM) (Model: HITACHI S-3400) attached with Energy dispersive spectroscopy (EDS).

III. RESULTS AND DISCUSSION

X-ray diffraction (XRD) patterns of pure and Ni (5% and 10%) doped ZnSe nanoparticles are shown in Fig.1. The diffraction peaks are indexed to the cubic phase of ZnSe with lattice constants of $a=5.618\text{\AA}$ [Joint Committee on Powder Diffraction Standards (JCPDS) card number 80-0021]. It is seen from the spectrum that the ZnSe nanoparticles exhibits the orientations along (1 1 1), (2 2 0), (3 1 1), (3 3 1) and (4 2 2) planes corresponding to the 2θ values given in Table I. The XRD peak intensity of the (111) plane was relatively higher than those of other reflections. The intensity of XRD peaks increases with the increase of Ni concentration from 5 to 10%. XRD data reveals that diffraction peaks of Ni doped ZnSe slightly shifts to the higher angle with increasing Ni concentration of 5% to ZnSe. It is due to the fact that the divalent Ni atoms occupy Zn^{2+} sites causing slight peak shifting of 0.24° towards higher angle in (1 1 1) peak giving rise to decrease in the interplanar spacing. The lattice parameter (a) for cubic structure were calculated by the following equation [17]

$$a = d (h^2 + k^2 + l^2)^{1/2} \quad (1)$$

Deformation cause local changes in atomic spacing are due to presence of uniform and non-uniform strain in the lattice parameters. In case of uniform strain, the interplanar lattice spacing shifts towards lower or higher value depends on the nature of the strain (tensile or compressive). In case of non uniform strain, there are changes in grain from one region to another within the regime. At higher doping concentration of Ni 10% in ZnSe, the interplanar lattice spacing shifts toward lower value, this leads to formation of tensile strain.

The average crystallite size (D) of pure and Ni doped ZnSe is obtained from the Scherer formula [18]

$$D = K\lambda/\beta\cos\theta \quad (2)$$

where λ , β and θ are the X-ray wavelength ($=0.154\text{ nm}$), full width of the XRD pattern peaks at half maximum (FWHM), and Bragg diffraction angle, respectively. The FWHM of diffraction peaks is found to be increased with increasing Ni^{2+} doping leading to decrease in the crystallite size. The crystallite size for the prepared samples is in the range of 40 - 67 nm.

The strain induced in crystals due to doping and distortion is calculated using the formula [19]

$$\varepsilon = \beta \cos \theta / 4 \quad (3)$$

The strain of the prepared samples increased from 0.746×10^{-3} to 0.826×10^{-3} $\text{line}^{-2} \text{m}^{-4}$ with the increase of Ni concentration in ZnSe. Table I depicts comparison of crystallite size and strain for undoped and Ni-doped ZnSe for 5 and 10% concentrations. It is clear that with both kind of concentration and doping, there was a decrease in crystallite size and an increase in strain level. Dislocation in the crystal represents defects or irregularity which may deleteriously affect the physical and chemical properties of the material. The dislocation density for the prepared sample has been determined using the equation [20]

$$\delta = 15\beta\cos\theta/4aD \quad (4)$$

where δ is dislocation density, β is broadening of diffraction line measured at half of its maximum intensity (in radian), θ is

Bragg's diffraction angle (in degree), while 'a' and 'D' are the lattice constant and crystallite size (in nm) respectively. The dislocation density of the samples increases from 1.83×10^{14} to $2.25 \times 10^{14} \text{ m}^{-2}$ with the increase of Ni doping concentration in ZnSe. The average internal stress S in the prepared samples can be determined using the following relation [21]:

$$S = [E/2\gamma] [(a_0-a)/ a_0] \quad (5)$$

where a_0 is the lattice parameters of the bulk material, E is the Young's modulus and γ is the Poisson's ratio of the films. Here 'a' refers to the lattice parameter of the prepared sample. The values of E and γ used in calculation however, are those of the bulk material of ZnSe. The average internal stress slightly increases with the increase of Ni doping in ZnSe nanoparticles. The microstructural parameters for pure and Ni doped ZnSe nanoparticles are given in Table II.

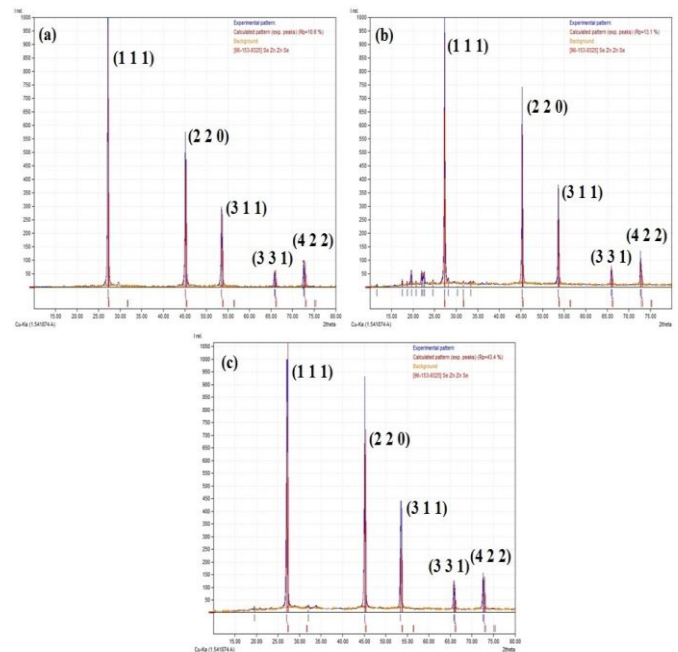


Fig. 1 XRD patterns of (a) pure ZnSe, (b) 5% Ni, (c) 10 % Ni doped ZnSe nanoparticles

FESEM images of un-doped and Ni doped ZnSe nanoparticles are shown in Figs. 2 (a, b and c). The surface morphology of pure and 5% Ni doped ZnSe nanoparticles confirm dense, less uniform size, agglomeration and nanometer scaled particles. Figure 2(c) shows the surface morphology of 10% Ni doped ZnSe, which represents a sort of clusters of nanoparticles on the surface. They were formed after aggregation of various grains. Figure 3(a) and 3(b) shows the EDS of pure ZnSe and 5% Ni doped ZnSe. Data analysis (i.e., atomic and weight percentage) from EDS patterns confirmed the stoichiometric composition of elements in the samples. For ZnSe nanoparticles, two elemental peaks related to Zn were found at ~ 1.0 and 8.6 keV , and one for Se at $\sim 1.4\text{ keV}$; whereas for 5% Ni doped ZnSe along with peaks related to Zn and Se, Fe peak is found at 0.85 and 7.46 keV respectively.

TABLE I : Structural properties of pure and Ni doped ZnSe nanoparticles

Sample	(h k l)	2θ	d-spacing, Å	FWHM (°)	Lattice constant, a (Å)	Crystallite size, D (nm)
ZnSe	(1 1 1)	27.17	3.2798	0.176	5.6807	46.4
	(2 2 0)	45.12	2.0074	0.174	5.6777	49.5
	(3 1 1)	53.51	1.7116	0.181	5.6767	49.1
	(3 3 1)	65.80	1.4182	0.209	6.1818	45.2
	(4 2 2)	72.58	1.3013	0.193	6.3750	51
ZnSe: Ni(5%)	(1 1 1)	27.41	3.2507	0.177	5.6303	46.2
	(2 2 0)	45.37	1.9969	0.149	5.6480	57.8
	(3 1 1)	53.74	1.7043	0.142	5.6525	62.7
	(3 3 1)	66.01	1.4140	0.161	6.1635	58.8
	(4 2 2)	72.79	1.2981	0.147	6.3593	67.1
ZnSe: Ni(10%)	(1 1 1)	27.20	3.2758	0.195	5.6740	42
	(2 2 0)	45.16	2.0060	0.213	5.6738	40.4
	(3 1 1)	53.53	1.7100	0.132	5.6714	67.4
	(3 3 1)	65.81	1.4179	0.192	6.1804	49.3
	(4 2 2)	72.59	1.3012	0.203	6.3745	48.5

TABLE III : Microstructural parameters of pure and Ni doped ZnSe nanoparticles

Sample	Micro strain, $\epsilon \times 10^{-3}$ (line ⁻² m ⁻⁴)	Dislocation density, $\delta \times 10^{14}$ (m ⁻²)	Average internal stress, $\times 10^{11}$ (Pa)
ZnSe	0.746	1.83	0.86
	0.700	2.64	2.18
	0.705	3.14	2.76
	0.765	4.47	3.58
	0.678	3.83	4.01
ZnSe: Ni(5%)	0.750	1.87	0.88
	0.600	1.94	2.20
	0.552	1.93	2.78
	0.590	2.65	3.60
	0.516	2.22	4.02
ZnSe: Ni(10%)	0.826	2.25	0.87
	0.858	3.97	2.18
	0.514	1.67	2.76
	0.703	3.77	3.58
	0.713	4.23	4.01

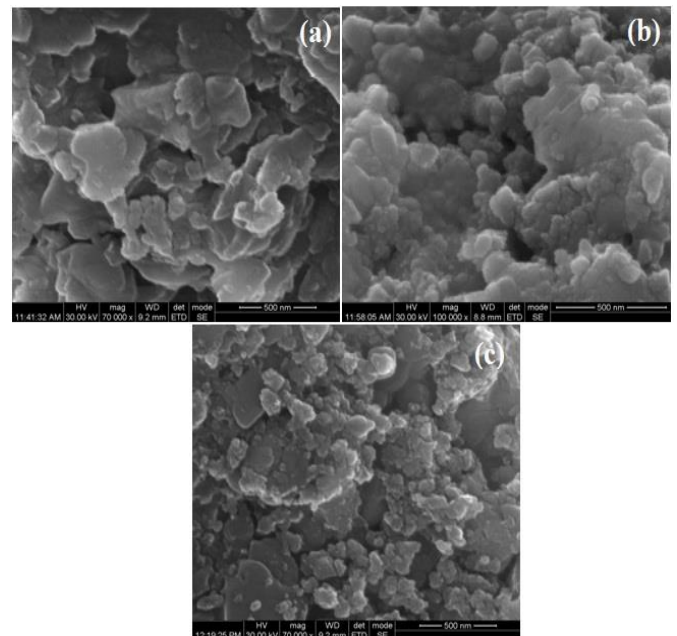


Fig. 2 FESEM images of (a) pure ZnSe, (b) 5% Ni, (c) 10% Ni doped ZnSe nanoparticles

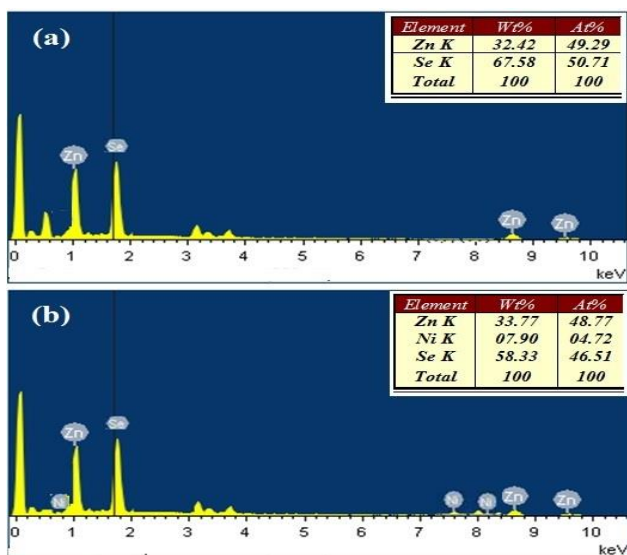


Fig. 3 EDS images of (a) pure ZnSe, (b) 5% Ni, (c) 10 % Ni doped ZnSe nanoparticles

IV. CONCLUSIONS

Pure and Ni doped ZnSe nanoparticles were successfully synthesized using the chemical co-precipitation method. XRD studies revealed that all the samples exhibit cubic phase. The crystallite size of the pure and Ni doped ZnSe nanoparticles are in the range of about 42- 46 nm. The crystallite-size decreases with the increase of Ni concentration in ZnSe. The microstructural parameters such as microstrain, dislocation density and internal stress of the prepared samples were discussed. The surface morphology of Ni doped ZnSe nanoparticles shows non-uniform size with agglomeration. EDS analysis confirms that the synthesized nanoparticles of ZnSe and Ni doped ZnSe do not contain any foreign element in them.

V. ACKNOWLEDGMENT

One of the author D. Subramanyam would like to thank University Grants Commission – South Eastern Regional office (UGC-SERO), Hyderabad for providing financial support under the minor research project No.F. MRP-4862/14(SERO-UGC).

REFERENCES

[1] Shenglin Xiong, Baojuan Xi, Chengming Wang, Guangcheng Xi, Xiaoyan Liu, and Yitai Qian, "Solution-Phase Synthesis and High Photocatalytic Activity of Wurtzite ZnSe Ultrathin Nanobelts: A General Route to 1D Semiconductor Nanostructured Materials," *Chem. Eur. J.* Vol. 13, pp. 7926 – 7932, (2007).

[2] X.D. Liu, J.M.Ma, P.Peng, and W.J.Meng, "Synthesis of hollow ZnSe nanospheres with high photocatalytic activity: synergetic effect of cation exchange and selective Cu_{2-x}Se template etching," *Langmuir*, Vol. 26 , pp. 9968-9973, 2010.

[3] P.T.K.Chin, J.W.Stouwdam, and R.A.J.Janssen, "Highly luminescent ultranarrow Mn doped ZnSe nanowires," *NanoLett.*, Vol. 9, pp 745-750, 2009.

[4] G.M. Lohar, R.K. Kamble, S.T. Punde, S. T. Jadhav, A.S. Patil, H.D. Dhaygude, B.P. Relekar, and V.J. Fulari, "Electrochemical Synthesis of Ni Doped ZnSe Thin Film for Photoelectrochemical Cell Application," *Materials Focus*, Vol. 5, pp.481-484, 2016

[5] Guoying Feng, Chao Yang, and Shouhuan Zhou, "Nanocrystalline Cr²⁺ doped ZnSe Nanowires laser," *Nano Lett.* Vol. 13, pp. 272-275, 2013.

[6] Melissa Cruz-Acuña, Sonia Bailón-Ruiz, Carlos R. Marti-Figueroa, Ricardo Cruz-Acuña, and Oscar J. Perales-Pérez, "Synthesis, Characterization and Evaluation of the Cytotoxicity of Ni-Doped Zn(Se,S) Quantum Dots," *Journal of Nanomaterials*, Vol. 2015, pp. 702391/1-8, 2015.

[7] A.P. Alivisatos, Semiconductor clusters," *Nanocrystals, and Quantum Dots*," *Science*, Vol. 271, pp. 933-937, 1996

[8] H. Luo, and J.K. Furdyna, "The II-VI semiconductor blue-green laser: challenges and solution," *Semicond. Sci. Technol.* Vol. 10, pp. 1041-1048, 1995

[9] P. Qi, Y.J. Dong and Y.D. Li, " ZnSe semiconductor hollow microspheres," *Angew. Chem. Int. Ed. Engl.* 42 , pp. 3027-3030, 2003

[10] A.R. Balu, V.S. Nagrethinam, M.G. Syed Basheer Ahamed, A. Thayumanavan, and K.R. Murali, "Influence of film thickness on the microstructural, Optoelectronic, morphological properties of nanocrystalline ZnSe thin films," *Mater. Sci. Eng. B*, Vol. 171, pp 93-98, 2010.

[11] M.G. Syed Basheer Ahamed, V.S. Nagrethinam, A.R. Balu, A. Thayumanavan, K.R. Murali, C. Sanjeeviraja, and M. Jayachandran, "Influence of substrate temperature on the properties of electron beam evaporated ZnSe film," *Cryst. Res. Technol.* Vol. 45, pp. 421-426, 2010.

[12] S. Chaliha , M.N. Borah, P.C. Sarmah, and A. Rahman, "Effect of substrate temperature on structural properties of thermally evaporated ZnSe thin films," *Optoelectron. and Adv. Mater.* Vol.10 , pp. 427-433, 2008.

[13] H. Fu, H. Li , W. Jie , and L. Yang, "The growth and characterization of ZnSe nanoneedles by a simple chemical vapor deposition method," *J. Cryst. Growth*, Vol. 289, pp. 440, 2006.

[14] M. Godlewski, M. Skrobot, E. Guziewicz , and M. Phillips, "Color tuning of white light emission from thin films of ZnSe.," *J. Lumin.* Vol. 125, pp. 85-91, 2007.

[15] R. Kowalik , P. Zabinski , and K. Fitzner, "Electrodeposition of ZnSe," *Electrochimica Acta*, Vol. 53, pp. 6184-6190, 2008.

[16] Y. Wang, X. Yao, M. Wang , F. Kong, and J. He, "Optical responses of ZnSe quantum dots in silica gel glasses," *J. Cryst. Growth*, Vol. 268 , pp 580-584, 2004.

[17] B. Rajesh Kumar, and T. Subba Rao, "Studies on structural and optical properties of vacuum evaporates In₂Te₃ thin films" *Chalcogenide Lett.* Vol. 8, pp. 83- 92, 2011.

[18] B. Hymavathi, B. Rajesh Kumar, and T. Subba Rao, "Temperature Dependent Structural and Optical Properties of Nanostructured Cr Doped CdO Thin Films Prepared by DC Reactive Magnetron Sputtering," *Procedia Mater. Sci.*, Vol.6, pp. 1668-1673, 2014.

[19] B. Hymavathi, B. Rajesh Kumar, and T. Subba Rao, *Mater. Today: Proceedings*, "Structural, Surface Morphological and Optical Properties of Cr Doped CdO Thin Films for Optoelectronic Devices," Vol. 2, pp. 1510-1517, 2015.

[20] Kanta Yadav, Y. Dwivedi, and Neena Jaggi, "Structural and optical properties of Ni doped ZnSe nanoparticles," *J. Lumin.* 158, pp. 181–187, 2015.

[21] C.K.De, and N. K. Misra, "X-ray diffraction analysis of lattice defects of ZnSe thin films deposited at different substrate temperatures," *Indian J. Phys.* 71A , pp. 535-544, 1997.